INTERNATIONAL JOURNAL OF
RADIATION ONCOLOGY • BIOLOGY • PHYSICS
www.redjournal.org

BRIEF REPORT

Timing of Planning Magnetic Resonance Imaging and Patient Selection for Adaptive Radiation Therapy in Newly Diagnosed High-Grade Glioma

Nicholas C. DeWalt, BS,[a] Theodore K. Yanagihara, MD, PhD,[b] Matthew Gallitto, MD, PhD,[c] Connor J. Kinslow, MD,[c] Codruta Chiuzan, PhD,[d] Yuanguang Xu, PhD,[c] Gagandeep Singh, MD,[e] Jeffrey N. Bruce, MD,[a] Tony J.C. Wang, MD,[c] and Jack Grinband, PhD[f,g]

[a]*Department of Neurological Surgery, Columbia University Irving Medical Center, New York, New York;* [b]*Department of Radiation Oncology, Lineberger Comprehensive Cancer Center, University of North Carolina, Chapel Hill, North Carolina;* [c]*Department of Radiation Oncology, Columbia University Irving Medical Center, New York, New York;* [d]*Institute of Health System Science, Feinstein Institutes for Medical Research, Northwell Health, New York, New York;* [e]*Department of Radiology, Neuroradiology Division, Columbia University Irving Medical Center, New York, New York;* [f]*Department of Radiology, Columbia University Irving Medical Center, New York, New York; and* [g]*Department of Psychiatry, Columbia University Irving Medical Center, New York, New York*

Received Dec 18, 2024; Revised Mar 13, 2025; Accepted for publication Mar 17, 2025

Purpose: Radiation therapy (RT) planning for high-grade glioma (HGG) typically relies on a single postoperative magnetic resonance image (MRI), assuming stable tumor and brain architecture throughout treatment. Though the gross tumor volume and surrounding tissues can shift after surgery and throughout RT, its rate of change, predictors of the movement magnitude, and impact on different dosing strategies are not well understood. This study uses meta-analysis and prospective MRI data to optimize MRI timing and identify patients who may benefit from adaptive RT (ART).

Methods and Materials: We performed a meta-analysis of 12 studies (405 patients) to quantify postresection brain morphology changes. Additionally, we prospectively collected MRIs from 17 newly diagnosed HGG patients who underwent resection and RT. Nonlinear image registration tracked voxel-wise movement from postsurgery through RT and follow-up. We analyzed changes in gross tumor volume, clinical target volume (CTV), and non-CTV influx volume (nCIV) across 8 CTV strategies. Exponential models predicted the magnitude and rate of postresection changes and optimal MRI timing.

Results: Both meta-analysis and prospective data showed that morphological changes followed an exponential decay, with 80% of shifts occurring within ∼30 days of resection. The nCIV was strongly predicted by T2-weighted fluid-attenuated inversion recovery volume and CTV margin strategy (86% accuracy for T1-based and 80% for T2-weighted fluid-attenuated inversion recovery-based CTVs). To minimize nCIV in patients starting RT >3 weeks postsurgery, our model suggests acquiring an additional MRI before RT. Otherwise, RT planning should be adaptive.

Corresponding author: Jack Grinband, PhD; E-mail: Jg2269@cumc.columbia.edu

Author responsible for statistical analysis: Jack Grinband, PhD; Email: Jg2269@cumc.columbia.edu

Tony J. C. Wang and Jack Grinband contributed equally.

Disclosures: This work was partially supported by the National Center for Advancing Translational Sciences, National Institutes of Health, through Grant Number UL1 TR000040. The content is solely the responsibility of the authors and does not necessarily represent the official views of the National Institutes of Health. This work was partially funded by a Varian Research Grant (IN004497), including salary support for T.J.C. W., J.G., and C.C.

Data Sharing Statement: Research data are stored in an institutional repository and will be shared upon request to the corresponding author.

Supplementary material associated with this article can be found in the online version at doi:10.1016/j.ijrobp.2025.03.037.

https://doi.org/10.1016/j.ijrobp.2025.03.037

Conclusions: Acquiring a delayed planning MRI or performing ART based on recent MRIs may optimize RT delivery for patients with larger tumors and specific CTV strategies. We propose a simple, clinically feasible algorithm for selecting patients and determining optimal MRI timing in prospective clinical trials of HGG ART.

Introduction

Adjuvant radiation therapy (RT) planning for newly diagnosed high-grade glioma (HGG) relies on a single postoperative magnetic resonance image (MRI) that is acquired within 48 hours after maximal safe resection.[1] This approach implicitly assumes that the tumor and surrounding brain architecture are static throughout treatment or that any intracranial movement does not significantly affect the radiation treatment field. The next MRI usually occurs 4 to 6 weeks post-RT completion to assess treatment response.

Studies have reported, however, that the gross tumor volume (GTV) and surrounding tissues can change in volume[2-5] and position[6,7] following surgery and throughout RT. Acquiring an additional MRI after the immediate postoperative MRI but before the start of RT or acquiring additional MRIs during RT for adaptive RT (ART) may help RT targeting if the GTV changes.[8-12] Although the acquisition of multiple MRIs was once impractical for RT planning and the turnaround time for generating radiation treatment plans was long, newer technology now makes ART feasible,[13] with ongoing clinical trials assessing its efficacy.[14,15]

Although ART has the potential to improve patient outcomes, there is limited understanding of which patient-specific factors predict the effectiveness of ART. Clinician decisions, such as including peritumoral edema in the GTV or alternative margin sizes, may impact the need for additional MRIs. Although a wide range of radiation dose strategies exist,[14] no studies have compared the potential benefit of ART across these methods. In addition, though some imaging-based studies suggest that most architectural changes occur during the first 20 fractions in a typical 30-fraction treatment,[6,7,16] the timing of these changes relative to tumor resection and the optimal time points for additional MRIs, if needed, is unknown.

We performed a meta-analysis to estimate the time course of morphological changes due to tumor resection. We then performed longitudinal imaging of newly diagnosed HGG during RT to measure the time course of postresection dynamics and to identify factors that predict which patients may benefit from ART. This study presents a method (1) to identify patients who have the potential to benefit from ART and (2) to offer guidance on the optimal timing of additional MRIs for RT planning following HGG resection.

Methods and Materials

GTV meta-analysis

We conducted a meta-analysis of the postresection changes in the GTV over time (Fig. 1) using the Preferred Reporting Items for Systematic Reviews and Meta-Analyses (PRISMA) 2020 recommendations (Figs. E1 and E2).[17] The review was not registered, and a protocol was not prepared. Studies measuring GTV changes over time were identified in March 2025 by searching Google Scholar for ("glioma" OR "glioblastoma" OR "GBM") AND ("radiation" OR "radiotherapy" OR "adaptive planning") AND ("postoperative changes" OR "tumor dynamics" OR "tumor migration" OR "treatment planning" OR "gross tumor volume" OR "serial imaging" OR "longitudinal"). The first 200 studies were screened. Included studies required (1) newly diagnosed HGG, (2) resection followed by RT, (3) measurements of the GTV relative to a baseline, (4) the time between surgery and measured GTV, (5) the radiographic definition of GTV, and (6) original studies rather than reviews. Two reviewers (N.C.D. and J.G.), working independently, identified 29 publications that addressed postoperative tumor volume changes. From these, 10 were excluded for not reporting the GTV relative to a baseline, and 3 were excluded for not reporting the time of imaging relative to surgery. Data from patients with progression before or during RT were excluded. Other exclusion reasons are shown in Figure E2. Additional information on the 12 included studies is in Table E1. The primary outcome measures were relative GTV, times of MRI acquisitions relative to surgery, and sample sizes. When absolute rather than relative GTVs were reported, each value was converted to a percentage of the GTV at the postoperative MRI. Outcomes were extracted from each study and recorded by N.D. and confirmed by J. G. Matlab (http://www.mathworks.com) was used to fit an exponential decay model to the relative GTV as a function of time. The fit was weighted by the sample size of each study, and 95% CIs were generated.

Meta-analysis bias assessment and sensitivity analysis

All included studies were observational and consisted of a single postoperative group; therefore, standard bias assessments, such as the Risk of Bias 2 Tool,[18] do not apply. Nevertheless, we individually assessed each study's bias.

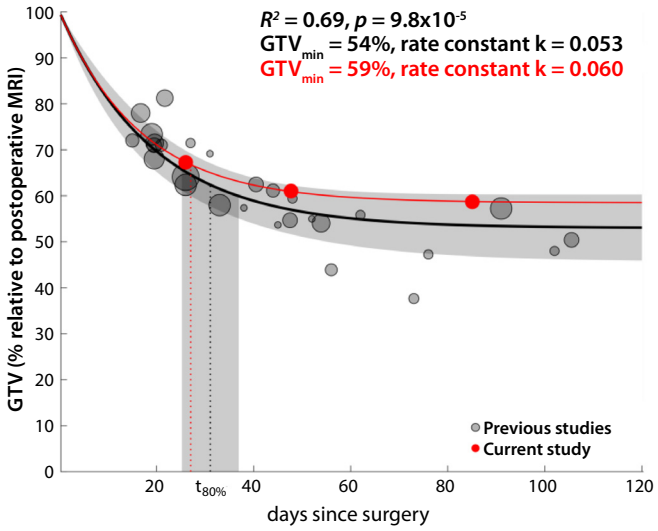

Fig. 1. Meta-analysis for the time course for GTV reduction following high-grade glioma resection. The size of each bubble is proportional to the patient sample size of the study. The curve estimate (solid line) and 95% CI (shaded regions) were weighted by study sample sizes. The 3 red data points correspond to the mean T1-GTV at the pre-RT MRI (MR_{pre}) the mid-RT MRI (MR_{mid}), and at the 1-month follow-up (MR_{fu}) relative to MR_{plan} for the current study data, along with the corresponding curve fit. The vertical lines $t_{50\%}$, $t_{80\%}$, and $t_{95\%}$ correlate to the times at which 50%, 80%, and 95% of the total GTV reduction had occurred, respectively. *Abbreviations:* GTV = gross tumor volume; MRI = magnetic resonance imaging.

Selection bias was considered low, as all studies included patients with newly diagnosed grade 3 or 4 gliomas (one study[9] had 4 grade 2 gliomas, which were excluded from the meta-analysis), thus yielding a relatively homogenous HGG data set. The risk of missing data was considered low for all studies, given that no study reported any loss to follow-up during the observation period, and dropout during standard-of-care RT for glioma is rare. One source of measurement bias is the inclusion of patients with early tumor progression (ie, prior to or during RT). When possible, we excluded data from these patients (eg, Bernchou et al,[6] Kraus et al,[19] and Végváry et al[20]). An assessment of each study's measurement bias is noted in Table E2. Another source of measurement error is the definition of the GTV — some studies defined GTV based on a contrast-enhanced T1-weighted MRI, while others used T2-weighted fluid-attenuated inversion recovery (T2-FLAIR). To address this, we conducted a subgroup analysis with the T1-based GTVs and T2-FLAIR-based GTVs separately. We also performed a sensitivity analysis in which the exponential fit was estimated using a leave-one-out procedure. Finally, we conducted a small-study effects analysis by estimating the exponential rate constant for each individual study and plotting the rate constant as a function of sample size.

Patient selection for prospective study

We prospectively collected MRI studies on 17 consecutive patients with newly diagnosed, pathology-proven HGG after surgical resection while undergoing RT and concurrent temozolomide from 2015 to 2017 (8 patients) and 2024 (9 patients). All patients included in the study provided consent as part of an institutional review board-approved study protocol. The median age at the time of surgery was 54 years (range, 28-74), with 10 men and 7 women. Ten patients had gross total resections (GTRs), and 7 had subtotal resections (STRs) that were considered "near-GTRs" because there was contrast enhancement located around the resection margins, which was indistinguishable from reactive enhancement due to surgical trauma. Additional diagnostic information on each patient is shown in Table E3.

Image acquisition

All patients obtained a postoperative MRI within 48 hours after surgery (MR_{plan}), including T1-weighted precontrast, T1-weighted postcontrast, and T2-FLAIR. The median time from the MR_{plan} to the start of RT was 27 days (range [SD], 13-50 [8.6]). Additional T1-weighted noncontrast images were acquired immediately before beginning RT (MR_{pre}) and 3 weeks into RT (MR_{mid}) for all patients. Ten patients had additional images acquired before and after each week of RT (totaling 7 MRIs during RT). Follow-up images after completion of RT (MR_{fu}) included the same sequences as the postoperative images. The median time from the end of RT to the MR_{fu} was 28 days (range [SD], 23-42 [5.9]). The imaging parameters are listed in Table E4.

Processing of image data

All imaging data was analyzed using the Functional Magnetic Resonance Imaging of the Brain (FMRIB) Software

Library (FSL). For each patient, structural images had all nonbrain voxels removed, were bias field (radio-frequency field inhomogeneity) corrected, and spatially coregistered to their respective MR_{plan} T1-weighted precontrast sequence using a linear, rigid body transform with 6 degrees of freedom and a correlation ratio cost function with FSL's Linear Image Registration Tool.[21] Nonlinear registration was then performed using FSL's Nonlinear Image Registration Tool to create warp fields, which describe the voxel-wise displacement of tissue from one time point to the next (Fig. 2A; additional examples in Fig. E3). This analysis assumes a 1-to-1 correspondence between images, meaning that any observed displacement is attributed solely to structural deformation rather than the emergence of new morphological features. Specifically, this approach does not account for potential changes such as the appearance of new contrast enhancement or new T2-FLAIR hyperintensities. Two physicians independently confirmed that no new contrast enhancement or T2-FLAIR hyperintensities were visible for any patients at MR_{fu}.

Radiation target delineation

GTVs were contoured on high-resolution MR_{plan} structural images. T1-GTV was defined as the resection cavity and any residual contrast enhancement based on the European SocieTy for Radiotherapy and Oncology (ESTRO)-European Association of Neuro-Oncology (EANO) protocol.[22] T2-FLAIR-GTV was defined as the resection cavity and surrounding regions of T2-FLAIR hyperintensity based on the NRG protocol.[23] Eight unique clinical target volumes (CTVs) were generated by isotropically expanding each GTV by 5, 10, 15, or 20 mm and excluding all nonbrain voxels.

Measures of morphological changes

Each warp field was applied to each GTV and CTV, generating updated targets at each subsequent time point. The new targets represent the new location of the original target after accounting for tissue movement, which can be compared with the target in the planning volume (ie, MR_{plan}) to assess volumetric changes over time. Three variables were measured. The non-CTV influx volume (nCIV) was defined at each time point as the volume of those voxels that began outside but migrated into the CTV (depicted in Fig. 2B and Fig. E3). The Dice coefficient, which provides a measure of overlap between the planning CTV and the updated CTV, was defined as follows:

$$\text{Dice} = \frac{2 \cdot |\text{CTV}_{\text{planning}} \cap \text{CTV}_{\text{updated}}|}{|\text{CTV}_{\text{planning}}| + |\text{CTV}_{\text{updated}}|}$$

where $|\text{CTV}_{\text{planning}}|$ and $|\text{CTV}_{\text{updated}}|$ are the number of voxels in the original and updated CTVs, respectively.

Time course analysis

To measure the time course of tumor dynamics, the nCIV, Dice coefficient, and GTV size were fit to exponential decay models. The nCIV was fit to the following equation, where $nCIV_{max}$ represents the horizontal asymptote, t represents the number of days since surgery, and k represents the time constant:

$$nCIV(t) = nCIV_{max}\left(1 - e^{-kt}\right)$$

The Dice coefficients and GTV size were fit to the rising exponentials where $Dice_{min}$ and GTV_{min} represent the horizontal asymptotes:

$$Dice(t) = Dice_{min} + (1 - Dice_{min})e^{-kt}$$

$$GTV_{vol}(\text{t}) = GTV_{min} + (1 - GTV_{min})\text{e}^{-\text{kt}}$$

To determine the time required for X percent of the maximum change to occur, t_x was isolated:

$$t_X = \frac{ln\left(1 - \frac{X}{100}\right)}{k}$$

For the nCIV and Dice coefficients, each patient's individual data were fit to a curve, and the resulting parameters A and k were averaged across patients to generate mean curves for each CTV. For the GTV meta-analysis, each study's reported relative GTV size was plotted against the time since surgery, and the fit was weighted by the sample size of each study.

Optimal adaptive MRI analysis

To determine the percentage of nCIV prevented with adaptive planning, we calculated the area under a representative nCIV curve from the start to the end of RT 6 weeks later, with the floor set as the value of nCIV(t) at the most recent MRI. This simulates adjusting the CTV to not include any tissue that was not originally in it based on the most recently acquired MRI. The percent reduction in cumulative nCIV exposure with additional imaging relative to without additional imaging was reported, as shown in Figure E4.

Statistical analysis

Statistical analyses and curve-fitting for nCIV, Dice coefficients, and GTV size were conducted using the MATLAB R2024b (The MathWorks, Inc.) Statistics and Machine Learning Toolbox, with statistical significance set at $P < .05$. Paired 2-tailed Student's t tests were used to compare time constants (k) and nCIV asymptotes (ie, $nCIV_{max}$) across different CTV strategies (within-subject) with the Bonferroni correction for multiple comparisons. To assess whether resection cavity or T2-FLAIR hyperintensity volume influenced the time course, linear regression analyses were

independently performed for each of the 8 CTV strategies tested using $t_{80\%}$, a log-transformed time constant k which represents the time required for 80% of the change to occur. The effect of resection cavity volume on the magnitude (ie, $nCIV_{max}$) of nCIV was also examined using linear regressions in a similar manner. Surface plots of nCIV as a function of GTV size and CTV margin were created based on a second-degree polynomial function.

Results

Meta-analysis of the time course of postresection dynamics

To estimate the time course of postresection architectural changes, we performed a meta-analysis of 12 previous studies,[4-9,11,16,19,20,24,25] consisting of a total of 405 patients (Figs. E1 and E2; Table E1), that have measured the GTV size relative to a planning MRI. The data were combined and fit to an exponential decay model, showing a fit with a $t_{80\%}$ of 30.2 ± 5.9 days (rate constant = 0.053 [0.045, 0.066], $R^2 = 0.69$, $p = 9.8 \times 10^{-5}$) (Fig. 1).

Selection bias and missing data bias were considered low for all studies (see Methods). A greater concern was measurement bias; most studies (n = 9) did not specify whether any patients showed tumor progression prior to or during RT. Since patients who underwent STRs are more likely to progress than those undergoing GTRs, we consider that at least some of the patients in our meta-analysis may have progressed during RT, which would reduce the rate of exponential decay. A second potential source of measurement bias was whether the GTV included T2-FLAIR hyperintensities. There were 7 studies (n = 272) that used T1-weighted MRI and 5 studies (n = 133) that used T2-FLAIR to define the GTV. We repeated an exponential fit with these 2 subgroups and found no significant difference (T1-based rate constant = 0.048 [0.037, 0.067] and T2-FLAIR-based rate constant = 0.043 [0.027, 0.104], $p = .76$). A sensitivity analysis using a leave-one-out approach found that the exclusion of only one study[25] caused a change in the exponential rate, decreasing from 0.053 [0.045, 0.066] to 0.042 [0.035, 0.054]. Finally, to test for small-study effects, we estimated the rate constant for each individual study and found that the rate constant was uncorrelated to sample size ($p = .28$).

Prospectively collected time course of postresection dynamics

Using our prospective data, we first tested whether the postresection architectural changes resulted in the GTV receiving less than the maximal dose of RT. The volume of tissue that began within the GTV and exited the CTV during RT was found to be small: with a 5 mm margin, T1-GTV movement caused 0.045%, 0.19%, and 0.90% of the GTV to be outside of the CTV at MR_{pre}, MR_{mid}, and MR_{fu}, respectively, while T2-FLAIR-GTV movement caused 0.033%, 0.11%, and 0.72% at the same time points, respectively. With a 10 mm margin or greater, no GTV voxels were outside of the CTV at any time (Fig. E5).

To characterize the rate of change in morphology, we overlaid the average T1-GTV size from our prospective study with the meta-analysis, which showed consistent results with a $t_{80\%}$ of 27.0 days (Fig. 1). We then measured the nCIV or the volume of surrounding tissue that enters the CTV over time. An example of the nonlinear registration with corresponding displacement vectors is shown in Figure 2A. Representative examples of morphological changes over time and the resulting nCIV accumulation are shown in Figure 2B and Figure E3. We tested 8 unique CTV configurations derived from 2 GTVs (T1-GTV and T2-FLAIR-GTV), each with 4 isotropic margin sizes (5, 10, 15, and 20 mm), as illustrated in Figure 3A. nCIV curves representing the group means are shown in Figure 3B. Exponential fits to each patient's nCIV are shown in Figure E6; across all fits, the median R^2 was 0.91 (IQR [0.88, 0.98]). The $t_{80\%}$ was 26.4 ± 3.2 days for the T1-GTV strategies and 29.7 ± 3.5 for the T2-FLAIR-GTV strategies. No significant differences in $t_{80\%}$ were found across different GTVs or margins ($P > .05$; paired t tests), and $t_{80\%}$ showed no association with GTV size in any of the 8 CTV strategies (maximum $R^2 = 0.05$, minimum $P = .37$). To further validate the time course, we fit curves to the Dice coefficients (Fig. E7), which demonstrated a $t_{80\%}$ of 26.6 ± 3.0 days for T1-GTV strategies and 30.0 ± 4.2 days for T2-FLAIR-GTV strategies, with a median R^2 of 0.92 (IQR [0.90, 0.98]) across all fits.

The values for $t_{50\%}$, $t_{80\%}$, and $t_{95\%}$, as well as the corresponding time constants for the nCIV curves, Dice curves, and GTV meta-analysis, are summarized in Figure 4A, which demonstrates consistent values across all measures. We calculated the percentage of cumulative nCIV that can be avoided with a single additional MRI (compared with using only a postoperative planning MRI) as a function of the start day of RT and the timing of the additional MRI (Fig. 4B). The model predicted that for patients beginning RT within 3 weeks of surgery, the optimal time for an additional MRI is during RT (depicted in Fig. 4B), but for those that start after 3 weeks, the optimal time is immediately preceding RT initiation. The predicted optimal times for 2, 3, and 4 additional MRIs are shown in Figure E8. The percentage of nCIV avoided with optimal timing for each number of MRIs is shown in Figure 4C, with a greater marginal benefit for additional MRIs in patients who start RT earlier rather than later.

Patient selection for additional imaging

Because the radiation plan can vary widely across hospitals, clinicians, and patients, we assessed how the GTV size and CTV strategy affect the magnitude of nCIV. Larger T2-FLAIR volumes were associated with higher nCIV (Fig. 5A).

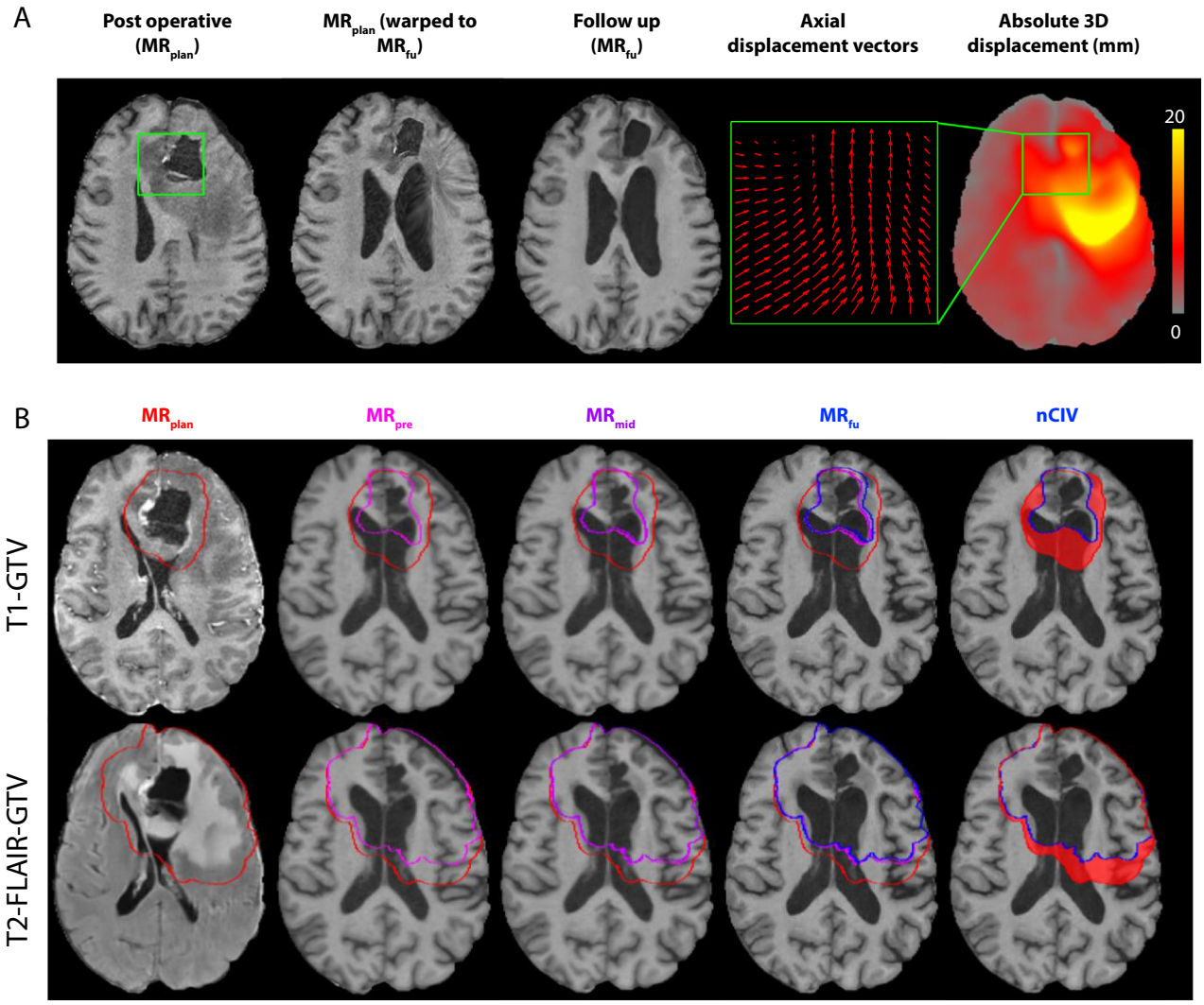

Fig. 2. Using nonlinear image registration to serially track postoperative architectural changes. (A) Nonlinear warping from planning magnetic resonance image (MRI) (MR_{plan}) to the follow-up MRI (MR_{fu}) for a 56-year-old male patient with GBM with associated displacement vectors for the region noted (green box) and displacement magnitude maps. (B) Serial changes in sample planning clinical target volumes (red; gross tumor volume [GTV] with 10 mm margins) for the same patient when they are warped to T1-GTV at the pre-RT MRI (MR_{pre}) (pink), the mid-RT MRI (MR_{mid},)(purple), and at the 1-month follow-up (MR_{fu}) (blue) time points. The nonclinical target volume influx volume (nCIV) at MR_{fu} is shaded in red. *Abbreviations:* 3D = 3 dimensional; T2-FLAIR = T2-weighted fluid-attenuated inversion recovery.

Notably, the T2-FLAIR volume better predicted the nCIV (mean R^2 = 0.72) than the resection cavity volume (mean R^2 = 0.49). Surfaces of nCIV were fit as a function of T2-FLAIR volume and CTV margin, with R^2 = 0.86 for T1-GTV strategies and R^2 = 0.80 for T2-FLAIR-GTV strategies (Fig. 5B). Larger margins were associated with a higher nCIV when using a T1-GTV (Fig. 5B, top) but a lower nCIV when using a T2-FLAIR-GTV (Fig. 5B, bottom). The effect of margin appeared to be greatest with larger tumors.

The relationship between CTV margin, resection cavity volume, and nCIV can be simplified into 2 clinically feasible algorithms to determine whether a patient would likely benefit from additional MRIs (Fig. 6A, B). Patients with a predicted nCIV > 35 cm^3 (the 70th percentile for our data) would acquire further imaging. A third algorithm is used to determine the optimal timing of the MRIs based on the start time of RT and the number of MRIs that will be acquired (Fig. 6C).

Discussion

Surgical resection of a newly diagnosed HGG can result in reliable displacements of brain morphology that continue throughout adjuvant RT. Our study is the first to (1) measure the rate of change of these morphological changes and (2) quantify the volume of tissue that migrates into the CTV following resection (ie, the nCIV). Our results culminate in

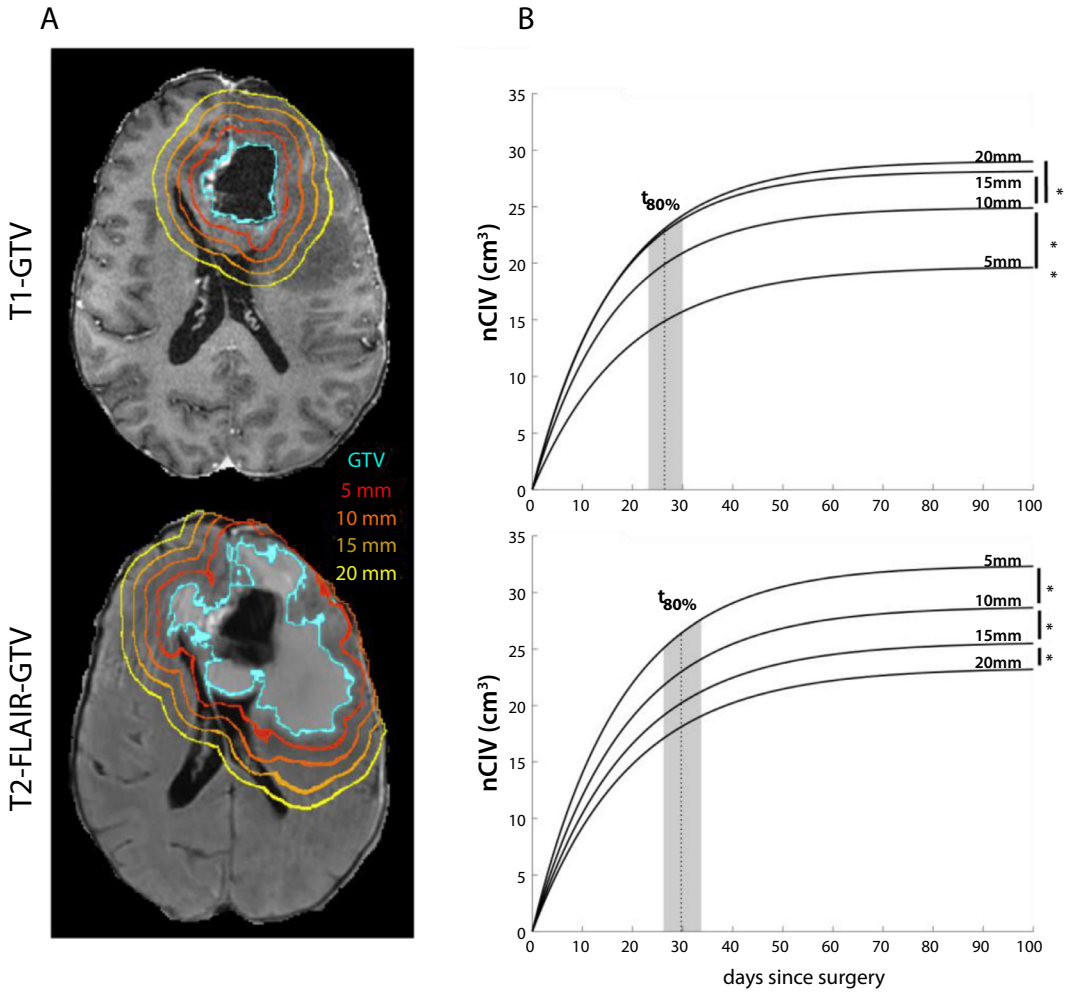

Fig. 3. Quantifying nonclinical target volume (CTV) influx volume (nCIV) over time. The upper row shows data for T1-gross tumor volume (GTV) plans; the lower row shows data for T2-weighted fluid-attenuated inversion recovery (T2-FLAIR)-GTV plans. (A) All sample CTVs tested with the corresponding GTVs are outlined in turquoise. CTVs were made with 5, 10, 15, and 20 mm margins, corresponding to red, red-orange, orange, and yellow outlines, respectively. (B) Exponential fits for the volume of nCIV entering each CTV over time following resection. The dotted vertical line and shaded regions correspond to the $t_{80\%}$ (which represents the time required for 80% of the change to occur) and its 95% CI, respectively. *Denotes statistically significant ($P < .05$) difference in nCIV asymptotes ($nCIV_{max}$) by paired t tests.

a proposed algorithm that may help clinicians decide when additional imaging is necessary to minimize the nCIV (Fig. 6A, B) and determine the optimal timing for those MRIs (Fig. 6C). The purpose of this algorithm is to assist in the design of future HGG ART prospective clinical trials.

Meta-analysis and time course

It has been previously shown that resection initiates rapid morphological changes that slow as the surgical cavity stabilizes and the edema resolves. Stewart et al[7] found that most target changes took place between fractions 10 and 20, while Bernchou et al[6] observed that the GTV size at fraction 10 correlated with follow-up values. Additionally, Cao et al[16] suggested that fraction 10 is the optimal time point for ART, as most changes have occurred by then compared with fraction 20. Kim and Lim[8] reported that after GTR, the resection cavity shrank more before RT than during RT. Our study is the first to characterize these changes using a mathematical model with data from the literature and our own longitudinal data collection.

Our meta-analysis summarized data over 12 studies comprising 405 patients (Fig. 1). The results were highly robust to outliers, the risk of selection bias was low, and there were no identifiable small-study effects. We also judge that there was a low risk of measurement error due to the definition of GTV because all studies used consistent definitions for within-subject, and we found no significant difference in the time course of morphological changes when comparing across differently defined GTV subgroups. However, this meta-analysis includes patients who underwent partial resections or biopsies only (ie, patients more likely to have tumor growth before and during RT that contributes to

A

	$t_{50\%}$(days)	$t_{80\%}$(days)	$t_{95\%}$(days)	Time constant (k)
nCIV (T1-GTV)	11.4 ±1.4	26.4 ±3.2	49.1 ±6.0	0.061 [0.054 0.069]
nCIV (T2-FLAIR-GTV)	12.8 ±1.5	29.7 ±3.5	55.3 ±6.5	0.054 [0.048 0.061]
Dice coefficient (T1-GTV)	11.4 ±1.3	26.6 ±3.0	49.5 ±5.6	0.061 [0.054 0.068]
Dice coefficient (T2-FLAIR-GTV)	13.3 ±1.8	31.0 ±4.2	57.6 ±7.9	0.052 [0.045 0.060]
GTV (meta-analysis)	13.0 ±2.5	30.2 ±5.9	56.2 ±10.9	0.053 [0.045 0.066]
GTV (current study)	11.6	27.0	50.3	0.060

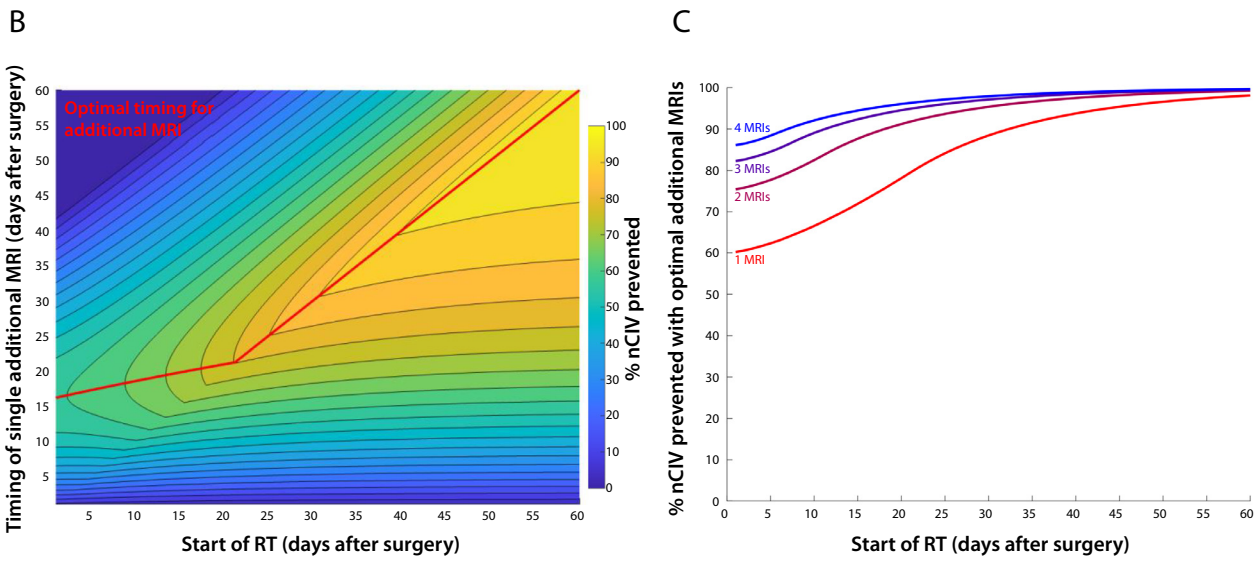

Fig. 4. Optimal additional magnetic resonance imaging (MRI) timing. (A) Summary of the time course of postresection tumor dynamics. (B) Percentage of nonclinical target volume influx volume (nCIV) that can be prevented with a single additional MRI scan as a function of the start day of radiation therapy (RT) and the timing of the additional MRI. The red curve corresponds to the optimal timing of the additional MRI that yields the maximum reduction in nCIV for the given RT start day. (C) The percentage of nCIV that can be prevented with 1, 2, 3, or 4 optimally timed additional MRIs as a function of the start day of RT. *Abbreviations:* GTV = gross tumor volume; T2-FLAIR = T2-weighted fluid-attenuated inversion recovery; t50%, t80%, and t95% correlate to the times at which 50%, 80%, and 95% of the total GTV reduction had occurred, respectively.

morphological changes). With 3 exceptions,[6,19,20] most studies did not report whether patients experienced detectable progression (novel contrast enhancement or edema) during RT. If we assume that at least some patients in the meta-analysis had unreported progression, then our estimated rate of change is likely to be slower than the unbiased estimate. As such, we assess the rate constant from the meta-analysis to be a lower bound and the true rate constant for patients without significant progression before or during RT to be higher, indicating more rapid tissue morphology changes.

Despite these biases, the rate of change in our GTV volume changes following resection closely matched the meta-analysis (Fig. 1), as well as the rates determined using the nCIV and the Dice coefficients (Fig. 4A), suggesting a robust final estimate. Interestingly, the rate of change was not associated with GTV size, indicating that other factors, such as cavity relaxation, resolution of T2-FLAIR hyperintensity/edema, cerebrospinal fluid production and ventricular expansion, ischemic changes, and scar tissue formation, may play significant roles.

The time course of postresection morphological changes has certain implications. Based on our model, acquiring a delayed planning MRI or obtaining adaptive MRIs during RT may assist with radiation treatment planning. The optimal RT start time after resection is unclear; however, some studies suggest that initiating RT at least 4 to 6 weeks after surgery may lead to the best outcomes for overall survival.[26-28] Our results suggest that for patients with large resections who start RT at least 3 weeks after surgery, acquiring an additional MRI immediately before RT may reduce radiation delivered to surrounding tissue outside the

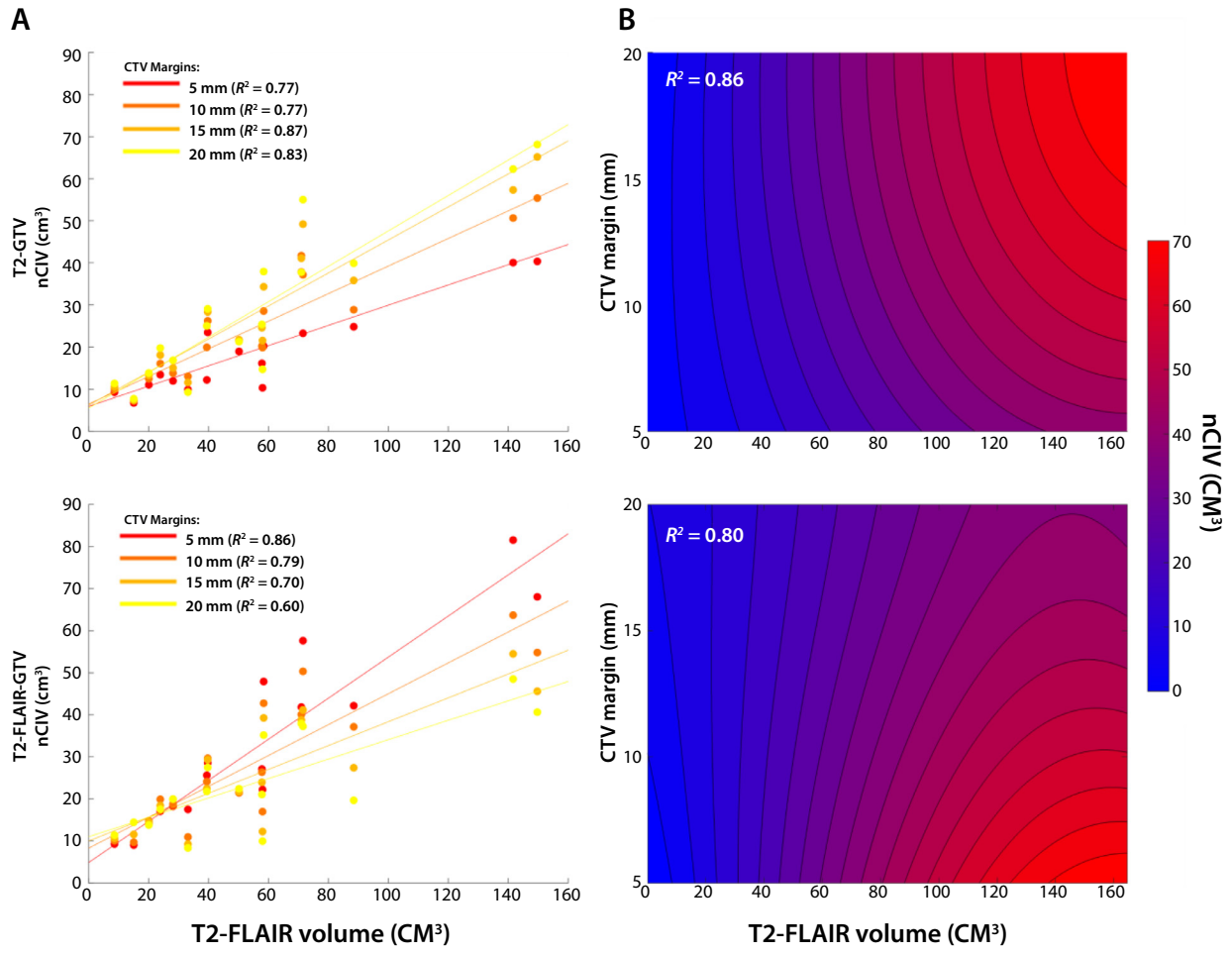

Fig. 5. T2-weighted fluid-attenuated inversion recovery (T2-FLAIR) volume and clinical target volume (CTV) margin strategy predict non-CTV influx volume (nCIV) magnitude. The upper row shows data for T1-gross tumor volume (GTV) plans; the lower row shows data for T2-FLAIR-GTV plans. (A) Linear regressions on the effect of T2-FLAIR size on nCIV. Each fit corresponds to a different CTV margin strategy, with 5, 10, 15, and 20 mm margins corresponding to red, red-orange, orange, and yellow outlines, respectively. (B) Surface fit for the volume of nCIV as a function of T2-FLAIR volume and CTV margin.

original CTV, while those who start RT earlier would benefit from adaptive imaging during RT (Fig. 4 and Fig. S6).

Patient selection for adaptive imaging

Obtaining an additional MRI after the immediate postoperative MRI for RT planning or performing ART may allow dose escalation to the target volume and reduce radiation dose outside the treatment volume. For example, Yang et al[9] reported that replanning radiation fields at the end of RT reduced the dose to organs at risk in 11 patients with gliomas, noting a larger difference with larger initial GTVs. A retrospective study by Kim and Lim[8] reported a reduction in normal brain irradiation when using an updated boost volume at week 5. Matsuyama et al[10] prospectively analyzed adaptive boost plans for 61 patients with GBM, demonstrating reduced radiation to organs at risk when using a mid-RT boost plan among patients who received a GTR.

A recent phase 2 trial demonstrated no increase in marginal failure rates when using a 5 mm CTV margin while acquiring weekly adaptive MRIs, demonstrating the safety and feasibility of adaptive planning.[15] Nonetheless, it has not been known which patients would benefit most from additional MRIs before RT or adaptive MRIs during RT. Our study introduces a new variable, nCIV, which represents brain tissue outside the original planning CTV that receives maximal radiation due to tissue movement. We found that nCIV is primarily predicted by the T2-FLAIR volume (Fig. 5A), consistent with Yang et al.[9] However, it is also affected by the CTV definition. For T1-based GTVs (eg, the ESTRO-EANO protocol),[22] increasing the CTV margins leads to an increase in nCIV, suggesting a potential benefit for additional MRIs. Conversely, for T2-FLAIR-based GTVs (eg, the NRG protocol),[23] increasing the margin decreases the nCIV, indicating a smaller impact of ART. Using the resection cavity volume and CTV margin strategy, we created a model to predict nCIV, which is able to explain 86%

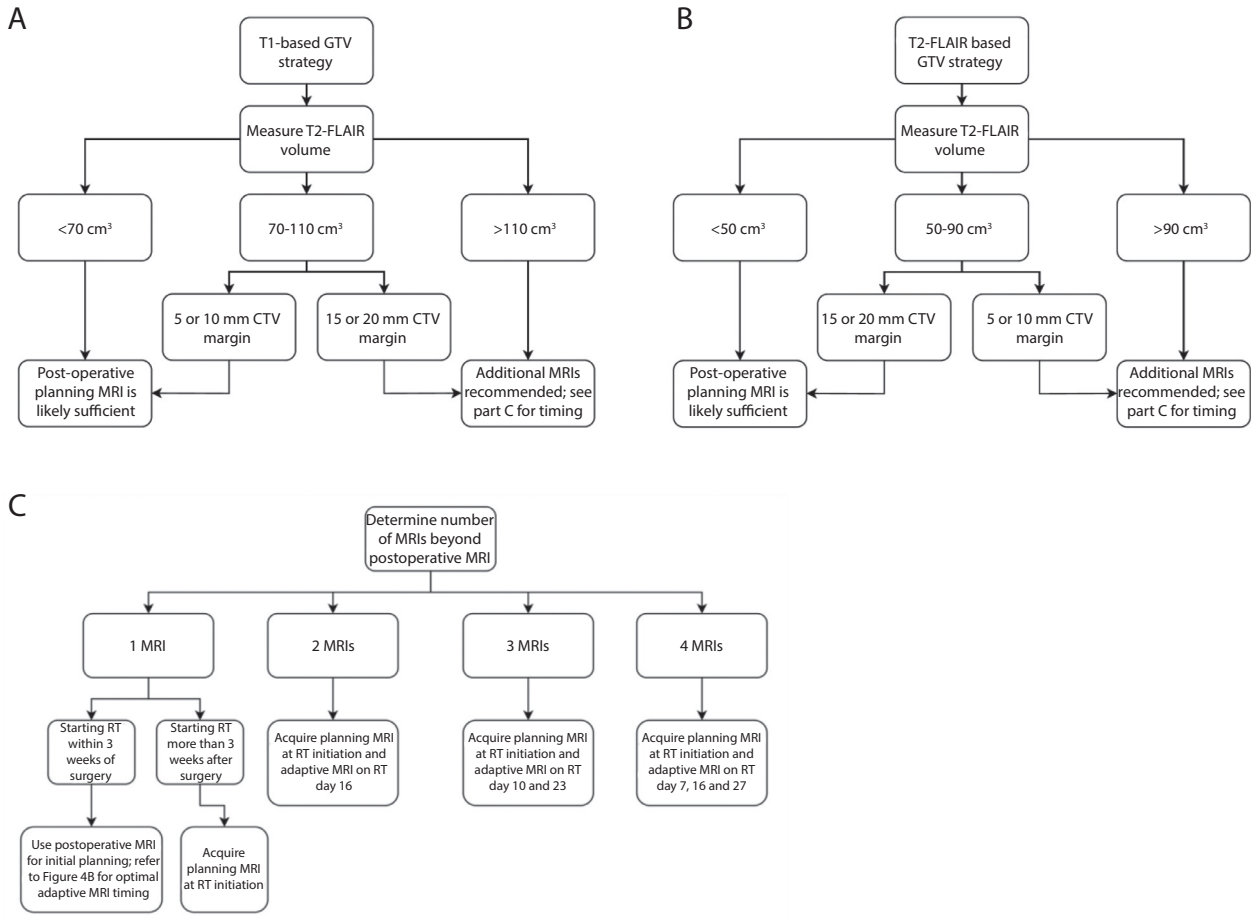

Fig. 6. Proposed algorithm for planning and adaptive magnetic resonance image (MRI) selections for newly diagnosed high-grade glioma radiation therapy (RT). Suggestions for selecting patients with high-grade glioma to receive additional MRIs based on (A) T1-based gross tumor volume (GTV) plans and (B) T2-weighted fluid-attenuated inversion recovery (T2-FLAIR)-based GTV plans. Note: both (A) and (B) use the T2-FLAIR volume for selecting patients. (C) Suggested timing for additional MRIs, including a delayed planning MRI or adaptive imaging. *Abbreviation:* CTV = clinical target volume.

of nCIV variance for T1-GTVs and 80% for T2-FLAIR-GTVs (Fig. 5B).

Our findings suggest that certain patients with newly diagnosed HGGs may benefit from additional imaging and that this depends on their resection cavity size and CTV contouring. This is an important consideration for future prospective HGG ART trials because the inclusion of patients who have little or no postsurgical architectural changes would reduce the likelihood of finding positive clinical outcomes for ART. We offer a simple algorithm to determine whether a patient may benefit from further imaging based on these factors (Fig. 6A, B). Though a clinically meaningful cutoff for nCIV values is not known, we decided to use the 70th percentile of our data, which corresponds to an nCIV of 35 cm^3 and represents the mean volume of a newly diagnosed GBM.[29] Further, Figure 6C provides recommendations for timing the RT planning MRI and adaptive MRIs, if they are to be acquired. Together, these recommendations can be used to optimize inclusion criteria and MRI timing for future prospective HGG ART trials.

Limitations

This study has several limitations, including a relatively small sample size, which may limit the identification of additional predictors for nCIV. For example, tumor location, such as the involvement of the corpus callosum, may influence GTV reduction and could improve our nCIV predictions.[25] Although our within-subject comparisons reliably measured exponential decay rates and were consistent across subjects, different volumetric measures, and previous studies, our findings will need to be validated in a larger prospective study. Another limitation is that we did not account for planning target volume margins, which range from 3 to 5 mm depending on the type of image guidance available and institutional preferences. Further, we only included patients who underwent GTR or near-GTR, where the main driver of changes is tissue removal and edema reduction rather than tumor progression. In patients undergoing STRs or biopsy only, the time course of changes could be driven by tumor growth, which may not follow an exponential decay.

Conclusions

Our study measures the time course of postresection morphological changes in patients with newly diagnosed HGGs, demonstrating that tissue migration may occur early and stabilize over time, consistent with a meta-analysis of 405 patients. Resection cavity volume and CTV margins are the most predictive factors in identifying who may benefit most from ART or additional planning MRIs. Optimal MRI timing, particularly acquiring an additional MRI immediately before RT for HGG patients with delayed treatment initiation, may improve radiation treatment planning. We provide a methodological framework for future prospective clinical trials using ART.

References

1. Tan AC, Ashley DM, López GY, Malinzak M, Friedman HS, Khasraw M. Management of glioblastoma: State of the art and future directions. *CA Cancer J Clin* 2020;70:299-312.
2. Manon R, Hui S, Chinnaiyan P, et al. The impact of mid-treatment MRI on defining boost volumes in the radiation treatment of glioblastoma multiforme. *Technol Cancer Res Treat* 2004;3:303-307.
3. Shukla D, Huilgol NG, Trivedi N, Mekala C. T2 weighted MRI in assessment of volume changes during radiotherapy of high grade gliomas. *J Cancer Res Ther* 2005;1:235-238.
4. Tsien C, Gomez-Hassan D, Ten Haken RK, et al. Evaluating changes in tumor volume using magnetic resonance imaging during the course of radiotherapy treatment of high-grade gliomas: Implications for conformal dose-escalation studies. *Int J Radiat Oncol Biol Phys* 2005;62:328-332.
5. Champ CE, Siglin J, Mishra MV, et al. Evaluating changes in radiation treatment volumes from post-operative to same-day planning MRI in high-grade gliomas. *Radiat Oncol* 2012;7:220.
6. Bernchou U, Arnold TST, Axelsen B, et al. Evolution of the gross tumour volume extent during radiotherapy for glioblastomas. *Radiother Oncol* 2021;160:40-46.
7. Stewart J, Sahgal A, Lee Y, et al. Quantitating interfraction target dynamics during concurrent chemoradiation for glioblastoma: A prospective serial imaging study. *Int J Radiat Oncol Biol Phys* 2021;109:736-746.
8. Kim TG, Lim DH. Interfractional variation of radiation target and adaptive radiotherapy for totally resected glioblastoma. *J Korean Med Sci* 2013;28:1233-1237.
9. Yang Z, Zhang Z, Wang X, et al. Intensity-modulated radiotherapy for gliomas:dosimetric effects of changes in gross tumor volume on organs at risk and healthy brain tissue. *Onco Targets Ther* 2016;9:3545-3554.
10. Matsuyama T, Fukugawa Y, Kuroda J, et al. A prospective comparison of adaptive and fixed boost plans in radiotherapy for glioblastoma. *Radiat Oncol* 2022;17:40.
11. Şenkesen Ö, Tezcanlı E, Abacıoğlu MU, et al. Limited field adaptive radiotherapy for glioblastoma: Changes in target volume and organ at risk doses. *Radiat Oncol J* 2022;40:9-19.
12. Kumar N, Kumar R, Sharma SC, et al. Impact of volume of irradiation on survival and quality of life in glioblastoma: A prospective, phase 2, randomized comparison of RTOG and MDACC protocols. *Neurooncol Pract* 2020;7:86-93.
13. Tseng CL, Chen H, Stewart J, et al. High grade glioma radiation therapy on a high field 1.5 Tesla MR-Linac - Workflow and initial experience with daily adapt-to-position (ATP) MR guidance: A first report. *Front Oncol* 2022;12:1060098.
14. Tseng CL, Zeng KL, Mellon EA, et al. Evolving concepts in margin strategies and adaptive radiotherapy for glioblastoma: A new future is on the horizon. *Neuro Oncol* 2024;26:S3-S16.
15. Detsky J, Chan AW, Palhares DM, et al. MR-linac on-line weekly adaptive radiotherapy for high grade glioma (HGG): Results from the UNITED single arm phase II trial. *Int J Radiat Oncol Biol Phys* 2024;120:S4.
16. Cao Y, Tang D, Xiang Y, et al. Study on the appropriate timing of postoperative adaptive radiotherapy for high-grade glioma. *Cancer Manag Res* 2021;13:3561-3572.
17. Page MJ, McKenzie JE, Bossuyt PM, et al. The PRISMA 2020 statement: An updated guideline for reporting systematic reviews. *BMJ* 2021;372:n71.
18. Sterne JAC, Savović J, Page MJ, et al. RoB 2: A revised tool for assessing risk of bias in randomised trials. *BMJ* 2019;366:l4898.
19. Kraus RD, Weil CR, Frances Su FC, Cannon DM, Burt LM, Mendez JS. Incidence and extent of disease progression on MRI between surgery and initiation of radiotherapy in glioblastoma patients. *Neurooncol Pract* 2022;9:380-389.
20. Végváry Z, Darázs B, Paczona V, et al. Adaptive radiotherapy for glioblastoma multiforme - The impact on disease outcome. *Anticancer Res* 2020;40:4237-4244.
21. Jenkinson M, Beckmann CF, Behrens TE, Woolrich MW, Smith SM. FSL. *Neuroimage* 2012;62:782-790.
22. Niyazi M, Andratschke N, Bendszus M, et al. ESTRO-EANO guideline on target delineation and radiotherapy details for glioblastoma. *Radiother Oncol* 2023;184:109663.
23. Kruser TJ, Bosch WR, Badiyan SN, et al. NRG brain tumor specialists consensus guidelines for glioblastoma contouring. *J Neurooncol* 2019;143:157-166.
24. Dejonckheere CS, Thelen A, Simon B, et al. Impact of postoperative changes in brain anatomy on target volume delineation for high-grade glioma. *Cancers (Basel)* 2023;15:2840.
25. Ong WL, Stewart J, Sahgal A, et al. Predictors of tumor dynamics over a 6-week course of concurrent chemoradiotherapy for glioblastoma and the effect on survival. *Int J Radiat Oncol Biol Phys* 2024;120:750-759.
26. Buszek SM, Al Feghali KA, Elhalawani H, Chevli N, Allen PK, Chung C. Optimal timing of radiotherapy following gross total or subtotal resection of glioblastoma: A real-world assessment using the National Cancer Database. *Sci Rep* 2020;10:4926.
27. Zur I, Tzuk-Shina T, Guriel M, Eran A, Kaidar-Person O. Survival impact of the time gap between surgery and chemo-radiotherapy in glioblastoma patients. *Sci Rep* 2020;10:9595.
28. Wang TJ, Jani A, Estrada JP, et al. Timing of adjuvant radiotherapy in glioblastoma patients: A single-institution experience with more than 400 patients. *Neurosurgery* 2016;78:676-682.
29. Henker C, Kriesen T, Glass Ä, Schneider B, Piek J. Volumetric quantification of glioblastoma: Experiences with different measurement techniques and impact on survival. *J Neurooncol* 2017;135:391-402.

Section and Topic	Item #	Checklist item	Location where item is reported
TITLE			
Title	1	Identify the report as a systematic review.	N/A
ABSTRACT			
Abstract	2	See the PRISMA 2020 for Abstracts checklist.	N/A
INTRODUCTION			
Rationale	3	Describe the rationale for the review in the context of existing knowledge.	Intro, para 4
Objectives	4	Provide an explicit statement of the objective(s) or question(s) the review addresses.	Intro, para 4
METHODS			
Eligibility criteria	5	Specify the inclusion and exclusion criteria for the review and how studies were grouped for the syntheses.	Methods, para 1
Information sources	6	Specify all databases, registers, websites, organisations, reference lists and other sources searched or consulted to identify studies. Specify the date when each source was last searched or consulted.	Methods, para 1
Search strategy	7	Present the full search strategies for all databases, registers and websites, including any filters and limits used.	Methods, para 1
Selection process	8	Specify the methods used to decide whether a study met the inclusion criteria of the review, including how many reviewers screened each record and each report retrieved, whether they worked independently, and if applicable, details of automation tools used in the process.	Methods, para 1
Data collection process	9	Specify the methods used to collect data from reports, including how many reviewers collected data from each report, whether they worked independently, any processes for obtaining or confirming data from study investigators, and if applicable, details of automation tools used in the process.	Methods, para 1
Data items	10a	List and define all outcomes for which data were sought. Specify whether all results that were compatible with each outcome domain in each study were sought (e.g. for all measures, time points, analyses), and if not, the methods used to decide which results to collect.	Methods, para 1
	10b	List and define all other variables for which data were sought (e.g. participant and intervention characteristics, funding sources). Describe any assumptions made about any missing or unclear information.	Methods, para 1
Study risk of bias assessment	11	Specify the methods used to assess risk of bias in the included studies, including details of the tool(s) used, how many reviewers assessed each study and whether they worked independently, and if applicable, details of automation tools used in the process.	Methods, para 2
Effect measures	12	Specify for each outcome the effect measure(s) (e.g. risk ratio, mean difference) used in the synthesis or presentation of results.	Methods, para 1
Synthesis methods	13a	Describe the processes used to decide which studies were eligible for each synthesis (e.g. tabulating the study intervention characteristics and comparing against the planned groups for each synthesis (item #5)).	Methods, para 1
	13b	Describe any methods required to prepare the data for presentation or synthesis, such as handling of missing summary statistics, or data conversions.	Methods, para 2
	13c	Describe any methods used to tabulate or visually display results of individual studies and syntheses.	N/A
	13d	Describe any methods used to synthesize results and provide a rationale for the choice(s). If meta-analysis was performed, describe the model(s), method(s) to identify the presence and extent of statistical heterogeneity, and software package(s) used.	Methods, para 2
	13e	Describe any methods used to explore possible causes of heterogeneity among study results (e.g. subgroup analysis, meta-regression).	Methods, para 2
	13f	Describe any sensitivity analyses conducted to assess robustness of the synthesized results.	Methods, para 2
Reporting bias assessment	14	Describe any methods used to assess risk of bias due to missing results in a synthesis (arising from reporting biases).	Methods, para 2
Certainty assessment	15	Describe any methods used to assess certainty (or confidence) in the body of evidence for an outcome.	Methods, para 2
RESULTS			
Study selection	16a	Describe the results of the search and selection process, from the number of records identified in the search to the number of studies included in the review, ideally using a flow diagram.	Flow diagram
	16b	Cite studies that might appear to meet the inclusion criteria, but which were excluded, and explain why they were excluded.	Table S1
Study	17	Cite each included study and present its characteristics.	Table S1

Section and Topic	Item #	Checklist item	Location where item is reported
characteristics			
Risk of bias in studies	18	Present assessments of risk of bias for each included study.	Table S1
Results of individual studies	19	For all outcomes, present, for each study: (a) summary statistics for each group (where appropriate) and (b) an effect estimate and its precision (e.g. confidence/credible interval), ideally using structured tables or plots.	Fig 1
Results of syntheses	20a	For each synthesis, briefly summarise the characteristics and risk of bias among contributing studies.	Results, para 2
	20b	Present results of all statistical syntheses conducted. If meta-analysis was done, present for each the summary estimate and its precision (e.g. confidence/credible interval) and measures of statistical heterogeneity. If comparing groups, describe the direction of the effect.	Results, para 1
	20c	Present results of all investigations of possible causes of heterogeneity among study results.	Results, para 2
	20d	Present results of all sensitivity analyses conducted to assess the robustness of the synthesized results.	Results, para 2
Reporting biases	21	Present assessments of risk of bias due to missing results (arising from reporting biases) for each synthesis assessed.	N/A
Certainty of evidence	22	Present assessments of certainty (or confidence) in the body of evidence for each outcome assessed.	Results, para 1,2
DISCUSSION			
Discussion	23a	Provide a general interpretation of the results in the context of other evidence.	Disc, para 2-5
	23b	Discuss any limitations of the evidence included in the review.	Disc, para 2-5
	23c	Discuss any limitations of the review processes used.	Disc, para 2-5
	23d	Discuss implications of the results for practice, policy, and future research.	Disc, para 8
OTHER INFORMATION			
Registration and protocol	24a	Provide registration information for the review, including register name and registration number, or state that the review was not registered.	Methods, para 1
	24b	Indicate where the review protocol can be accessed, or state that a protocol was not prepared.	Methods, para 1
	24c	Describe and explain any amendments to information provided at registration or in the protocol.	N/A
Support	25	Describe sources of financial or non-financial support for the review, and the role of the funders or sponsors in the review.	Acknowledgements
Competing interests	26	Declare any competing interests of review authors.	Conflicts
Availability of data, code and other materials	27	Report which of the following are publicly available and where they can be found: template data collection forms; data extracted from included studies; data used for all analyses; analytic code; any other materials used in the review.	Available upon request

Figure S1. 2020 Prisma checklist.

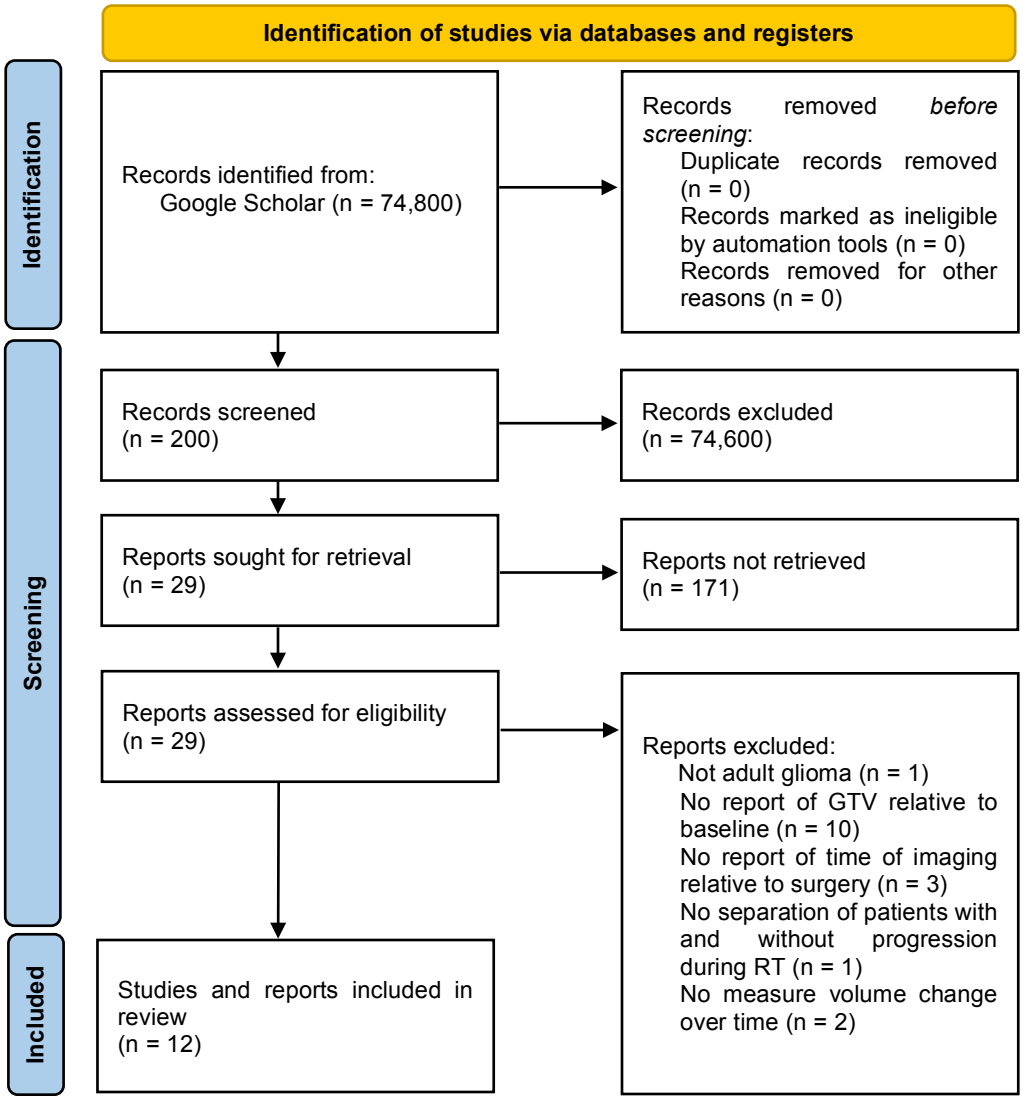

Figure S2. Prisma flow chart.

Study	Year	Subjects included	Tumors included	GTV definition	Time points used (days after resection)	GTV (relative to baseline)
Bernchou et al	2021	10	GBM	T1w	27, 48, 62, 76, 102	0.72, 0.60, 0.56, 0.47, 0.48
Cao et al	2021	10	HGG	T1w	31, 38, 45, 52	0.69, 0.57, 0.54, 0.55
Champ et al	2012	24	HGG	T2-FLAIR	17	0.78
Dejonckheere et al	2023	28	HGG	T2-FLAIR	20	0.68
Kim et al	2013	19	GBM	T1w	21, 56	0.71, 0.44
Kraus et al	2022	50	GBM	T2-FLAIR	26	0.64
Ong et al	2024	129	GBM	T1w	19, 26, 33, 91	0.73, 0.62, 0.58, 0.57
Senkesen et al	2022	24	GBM	T2-FLAIR	15, 44	0.72, 0.61
Stewart et al	2021	61	GBM	T1w	20, 41, 48, 106	0.71, 0.63, 0.55, 0.50
Tsien et al	2005	19	GBM	T1w	22	0.81
Vegvary et al	2020	24	GBM	T1w	20, 53	0.72, 0.54
Yang et al	2016	7	HGG	T2-FLAIR	73	0.38

Table S1. Studies reporting GTV change relative to date of surgery.

GBM = glioblastoma
HGG = high-grade glioma

Study	Sample size	Percent of patients who underwent GTR	Percent of patients who underwent STR	Percent of patients who underwent biopsy	Does the study separate patients with early growth?	Overall assessment of measurement bias
Bernchou et al	29	45	31	24	Yes	Low
Cao et al	10	60	40	0	No	Low
Champ et al	24	17	79	4	No	Medium
Dejonckheere et al	28	Unreported	Unreported	Unreported	No	High
Kim et al	19	100	0	0	No	Low
Kraus et al	50	36	64*	64*	Yes	Low
Ong et al**	129	29	55	15	No	Medium
Senkesen et al	24	58	25	17	No	Low
Stewart et al	61	30	57	13	No	Medium
Tsien et al	19	0	43	57	No	High
Vegvary et al	43	21	63	16	Yes	Low
Yang et al	7	43	57	0	No	Medium

Table S2. Summary of measurement bias. GTR = gross total resection, STR = subtotal resection. Sample size refers to the entire study's sample size, even if only a subset of data was used for the meta-analysis. Measurement bias assessment was based on the relative proportions of GTR, STR, and biopsy. The high-risk studies either did not report the relative proportions or had a majority of biopsy-only. The medium-risk studies had a majority of STRs while the low-risk studies had a majority of GTRs or separated patients with early growth.

*Kraus et al combined STR and biopsy into a single group.
**Ong et al had a single subject not undergo any resection, however, given the large sample size (n = 129), it was concluded that this was unlikely to have any meaningful impact on the meta-analysis.

Patient ID	Age at surgery	Sex	Diagnosis	Tumor location	Time from MRI_{plan} to start of RT (days)	Time from end of RT to MRI_{fu} (days)	T1-GTV (cm^3)	T2-FLAIR-GTV (cm^3)	Surgical outcome
1	59	M	GBM	R temporal	15	33	20.3	58.4	STR
2	74	F	GBM	L temporal	13	41	5.3	33.1	GTR
3	70	M	GBM	R temporal	23	32	28.5	88.4	GTR
4	28	M	GBM	L temporal	25	38	19.6	39.7	GTR
5	45	M	GBM	L frontal	25	28	10.0	58.0	STR
6	49	M	GBM	L parietal	20	23	9.1	39.4	GTR
7	54	M	GBM	L temporal	25	28	51.1	149.7	STR
8	68	F	GBM	L parietal	13	42	4.0	15.0	STR
9	56	M	GBM	L frontal	50	30	29.6	141.6	GTR
10	68	F	GBM	L frontal	30	27	6.5	20.0	STR
11	45	M	Astrocytoma, grade III, IDH-mutant	R frontal	29	28	37.7	50.1	GTR
12	41	F	GBM	R parietooccipital	27	27	17.9	57.8	GTR
13	31	M	Astrocytoma, grade IV, IDH-wildtype	R frontal	30	24	16.5	23.8	GTR
14	50	F	GBM	R frontal	29	25	32.0	70.9	GTR
15	60	F	GBM	L temporooccipital	28	30	8.6	8.6	STR
16	59	M	GBM	R frontal	30	NA	5.1	71.5	GTR
17	42	F	GBM	R temporoparietal	30	NA	3.6	28.1	STR
Median	**54**				**27**	**31**	**16.5**	**48.9**	

Table S3: **Patient demographic and tumor characteristics**. GBM = glioblastoma; IDH = isocitrate dehydrogenase; GTR = gross total resection; STR = subtotal resection. Note: All STRs were near-total resections and were labeled STR because contrast-enhancement at the resection margins were indistinguishable from reactive enhancement due to surgical trauma.

Time point	Sequence	Subject	Acquisition Type	Rows	Columns	Slice Thickness (mm)	TR (ms)	Flip Angle	TE (ms)	Manufacturer	Model	Field Strength (T)
Planning MRI (MR_p)	T1pre	1	3D	120	512	1.40	9	13	4	GE	Signa HDxt	3.0
		2		120	512	1.40	9	13	4	GE	Signa HDxt	3.0
		3		128	512	1.40	9	13	4	GE	Signa HDxt	3.0
		4		288	512	1.20	8	12	3	GE	Signa HDxt	3.0
		5		114	512	1.40	10	13	4	GE	Signa HDxt	1.5
		6		248	512	1.20	8	12	3	GE	Signa HDxt	3.0
		7		114	512	1.40	9	13	4	GE	Signa HDxt	1.5
		8		120	512	1.40	9	13	4	GE	Signa HDxt	3.0
		9		328	512	1.00	8	13	3	GE	Signa HDxt	1.5
		10		160	512	1.00	7	13	3	GE	SIGNA Premier	3.0
		11		168	1024	0.25	6	13	3	GE	SIGNA Premier	3.0
		12		512	512	1.00	6	13	2	GE	SIGNA Premier	3.0
		13		512	512	1.00	6	13	3	GE	SIGNA Premier	3.0
		14		512	512	2.00	8	13	3	GE	Signa HDxt	1.5
		15		512	512	1.00	6	13	2	GE	SIGNA Premier	3.0
		16		512	512	1.00	6	13	2	GE	SIGNA Premier	3.0
		17		512	512	1.00	6	13	2	GE	SIGNA Premier	3.0
	T1post	1	3D	120	512	1.40	9	13	4	GE	Signa HDxt	3.0
		2		120	512	1.40	9	13	4	GE	Signa HDxt	3.0
		3		128	512	1.40	9	13	4	GE	Signa HDxt	3.0
		4		288	512	1.20	8	12	3	GE	Signa HDxt	3.0
		5		114	512	1.40	10	13	4	GE	Signa HDxt	1.5
		6		248	512	1.20	8	12	3	GE	Signa HDxt	3.0
		7		114	512	1.40	9	13	4	GE	Signa HDxt	1.5
		8		120	512	1.40	9	13	4	GE	Signa HDxt	3.0
		9		328	512	1.00	8	13	3	GE	Signa HDxt	1.5
		10		160	512	1.00	7	13	3	GE	SIGNA Premier	3.0
		11		168	1024	0.25	6	13	3	GE	SIGNA Premier	3.0
		12		512	512	1.00	6	13	2	GE	SIGNA Premier	3.0
		13		512	512	1.00	6	13	3	GE	SIGNA Premier	3.0
		14		512	512	2.00	8	13	3	GE	Signa HDxt	1.5
		15		512	512	1.00	6	13	2	GE	SIGNA Premier	3.0
		16		512	512	1.00	6	13	2	GE	SIGNA Premier	3.0
		17		512	512	1.00	6	13	2	GE	SIGNA Premier	3.0
	T2-FLAIR	1	2D	512	512	5.00	9502	90	125	GE	Signa HDxt	3.0
		2		512	512	5.00	9502	90	122	GE	Signa HDxt	3.0
		3		512	512	5.00	9000	90	123	GE	Signa HDxt	3.0
		4		512	512	5.00	9000	90	135	GE	Signa HDxt	3.0
		5		256	256	5.00	8800	90	121	GE	Signa HDxt	1.5
		6		512	512	5.00	9000	90	132	GE	Signa HDxt	3.0
		7		512	512	4.00	8800	90	128	GE	Signa HDxt	1.5
		8		512	512	5.00	9502	90	124	GE	Signa HDxt	3.0
		9		256	256	3.00	9150	90	108	GE	Signa HDxt	1.5
		10		512	512	3.00	8300	160	88	GE	SIGNA Premier	3.0
		11		1024	1024	3.00	11000	160	92	GE	SIGNA Premier	3.0
		12		640	640	6.50	10000	90	105	Toshiba	Titan	1.5
		13		1024	1024	3.00	9000	160	92	GE	SIGNA Premier	3.0
		14		256	256	3.00	8800	90	109	GE	Signa HDxt	1.5
		15		1024	1024	3.00	9000	160	93	GE	SIGNA Premier	3.0
		16		512	512	4.00	9000	160	91	GE	SIGNA Premier	3.0
		17		512	512	4.00	9000	160	89	GE	SIGNA Premier	3.0
Non-clinical MRIs (during RT)	T1pre	1-8	3D	128	128	2.00	4.33	8	2	Philips Medical Systems	Achieva	3.0
		9-17		512	512	0.50	65	13	26	GE	SIGNA Premier	3.0
Follow up MRI (MR_{fu})	T1pre	1	3D	108	512	0.50	9	13	4	GE	Signa HDxt	1.5
		2		150	512	0.50	18	30	2	Philips Medical Systems	Achieva	3.0
		3		155	512	0.50	22	30	6	Philips Medical Systems	Intera	1.5
		4		160	256	1.00	8	12	3	GE	Signa HDxt	1.5
		5		114	512	0.50	9	13	4	GE	Signa HDxt	1.5
		6		160	256	1.00	8	12	3	GE	Signa HDxt	1.5
		7		120	512	0.50	8	8	3	Philips Medical Systems	Intera	1.5
		8		150	512	0.50	18	30	2	Philips Medical Systems	Achieva	3.0
		9		154	826	0.25	6	13	2	GE	SIGNA Premier	3.0
		10		168	1024	1.25	6	13	2	GE	SIGNA Premier	3.0
		11		168	1024	0.25	6	13	2	GE	SIGNA Premier	3.0
		12		512	512	1.00	6	13	2	GE	SIGNA Premier	3.0
		13		512	512	1.00	6	13	2	GE	SIGNA Premier	3.0
		14		512	512	1.00	6	13	2	GE	SIGNA Premier	3.0
		15		512	512	1.00	6	13	2	GE	SIGNA Premier	3.0

	T1post	**1**	3D	108	512	0.50	9	13	4	GE	Signa HDxt	1.5
		2		150	512	0.50	18	30	2	Philips	Achieva	3.0
		3		155	512	0.50	22	30	6	Philips	Intera	1.5
		4		160	256	1.00	8	12	3	GE	Signa HDxt	1.5
		5		114	512	0.50	9	13	4	GE	Signa HDxt	1.5
		6		160	256	1.00	8	12	3	GE	Signa HDxt	1.5
		7		120	512	0.50	8	8	3	Philips	Intera	1.5
		8		150	512	0.50	18	30	2	Philips	Achieva	3.0
		9		512	512	1.00	6	13	2	GE	SIGNA Premier	3.0
		10		168	1024	0.25	6	13	2	GE	SIGNA Premier	3.0
		11		168	1024	0.25	6	13	2	GE	SIGNA Premier	3.0
		12		512	512	1.00	6	13	2	GE	SIGNA Premier	3.0
		13		512	512	1.00	6	13	2	GE	SIGNA Premier	3.0
		14		512	512	1.00	6	13	2	GE	SIGNA Premier	3.0
		15		512	512	1.00	6	13	2	GE	SIGNA Premier	3.0
	T2-FLAIR	**1**	2D	256	256	5.00	8800	90	128	GE	SignaHDxt	1.5
		2		560	560	5.00	11000	90	125	Philips	Achieva	3.0
		3		1024	1024	5.00	8000	90	120	Philips	Intera	1.5
		4		512	512	5.00	8800	90	125	GE	Signa HDxt	1.5
		5		256	256	5.00	8800	90	126	GE	Signa HDxt	1.5
		6		512	512	5.00	8800	90	124	GE	Signa HDxt	1.5
		7		512	512	4.00	8000	90	102	Philips	Intera	1.5
		8		560	560	5.00	11000	90	125	Philips	Achieva	3.0
		9		1024	1024	3.00	9000	160	91	GE	SIGNA Premier	3.0
		10		1024	1024	3.00	9000	160	89	GE	SIGNA Premier	3.0
		11		1024	1024	3.00	7200	160	92	GE	SIGNA Premier	3.0
		12		1024	1024	3.00	9000	160	93	GE	SIGNA Premier	3.0
		13		1024	1024	3.00	9000	160	92	GE	SIGNA Premier	3.0
		14		1024	1024	3.00	9000	160	93	GE	SIGNA Premier	3.0
		15		1024	1024	3.00	9000	160	92	GE	SIGNA Premier	3.0

Table S4: Image acquisition parameters.

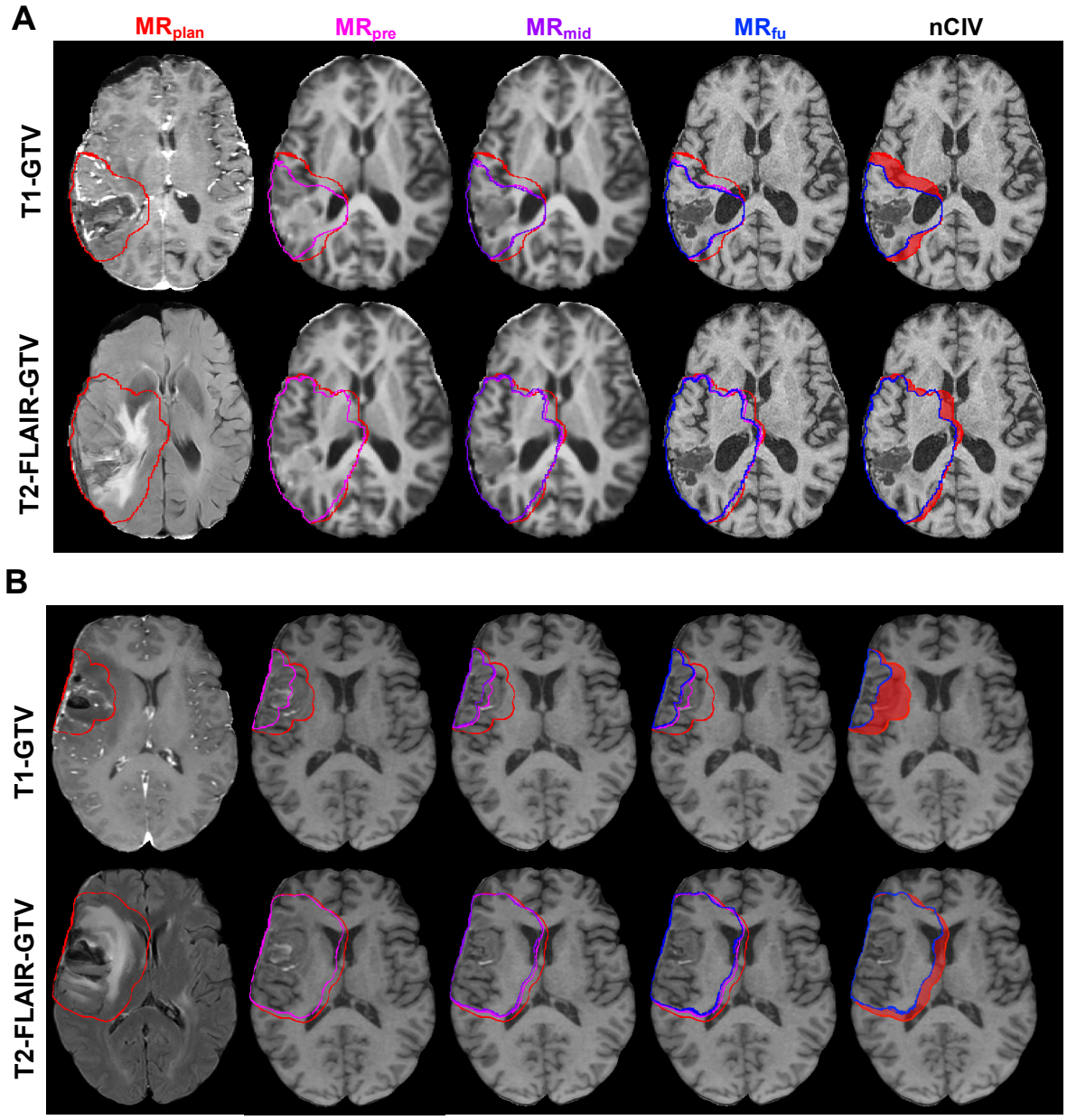

Figure S3. Additional examples of serially tracking post-operative architectural changes. Serial changes in sample planning CTVs (red; GTV with 10 mm CTV margins) when they are warped to MR_{pre} (pink), MR_{mid} (purple), and MR_{fu} (blue) timepoints. The nCIV at MR_{fu} is shaded in red. **(A)** 70-year-old male with GBM and **(B)** 59-year-old male with GBM.

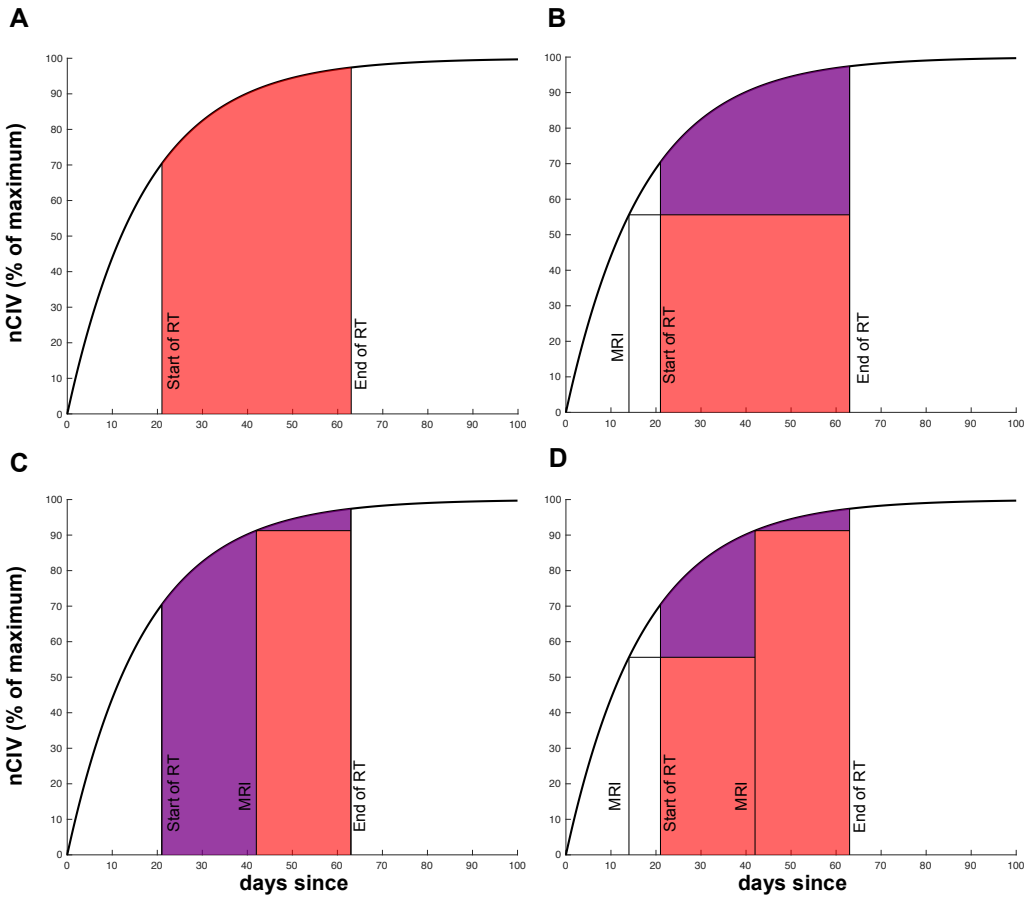

Figure S4. Sample scenarios for calculating percentage of cumulative nCIV avoided with additional MRIs. A sample nCIV curve is shown in each scenario demonstrating the time course. **(A)** The red shaded area indicates the cumulative nCIV volume and time spent in the CTV during radiation without any additional MRIs beyond the post-operative scan. The purple areas represent the cumulative nCIV if additional MRIs are taken **(B)** one week prior to the start of RT, **(C)** at the midpoint of RT, **(D)** one week prior to the start and at the midpoint of RT. The percentage reduction from the red (no additional imaging) to the purple (additional imaging) is calculated. All samples show RT beginning on post-operative day 21.

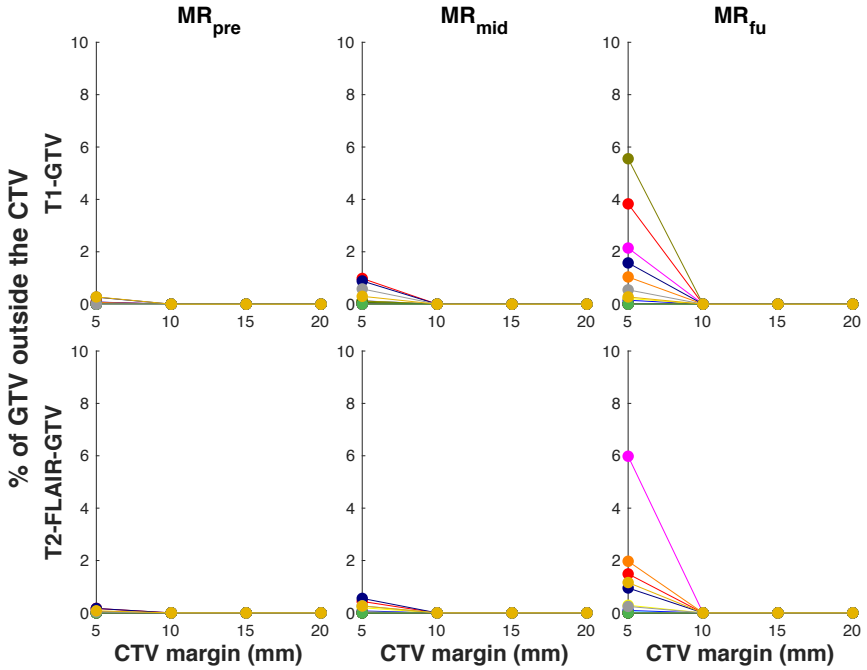

<u>Figure S5</u>. GTV coverage is nearly complete with 5 mm CTV margins and complete with 10 mm CTV margins or greater. The percent of GTV that migrates outside of the CTV with various margins is shown. The top row shows T1-GTV strategies while the bottom row shows T2-FLAIR-GTV strategies. The columns from left to right show each time point (MR_{pre}, MR_{mid}, and MR_{fu}).

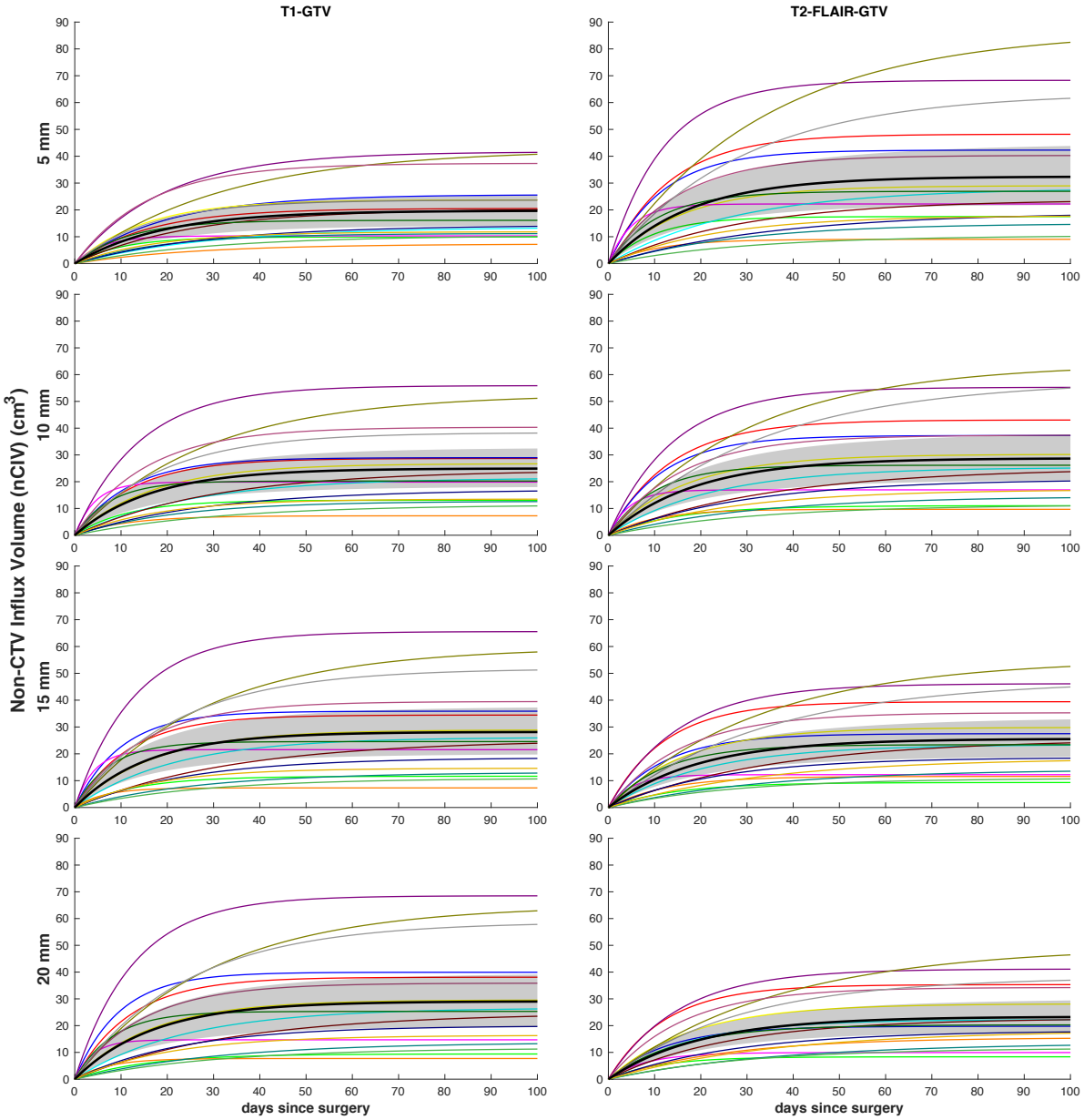

<u>Figure S6</u>. Individual GBM patient and composite nCIV curves for eight CTVs tested. Left column is 4 CTVs based on the T1-GTV; right column is 4 CTVs based on T2-FLAIR-GTV. Each color corresponds to a single patient. Each patient's time constant and asymptote were averaged to generate composite curves (black lines) and 95% confidence intervals (shaded regions).

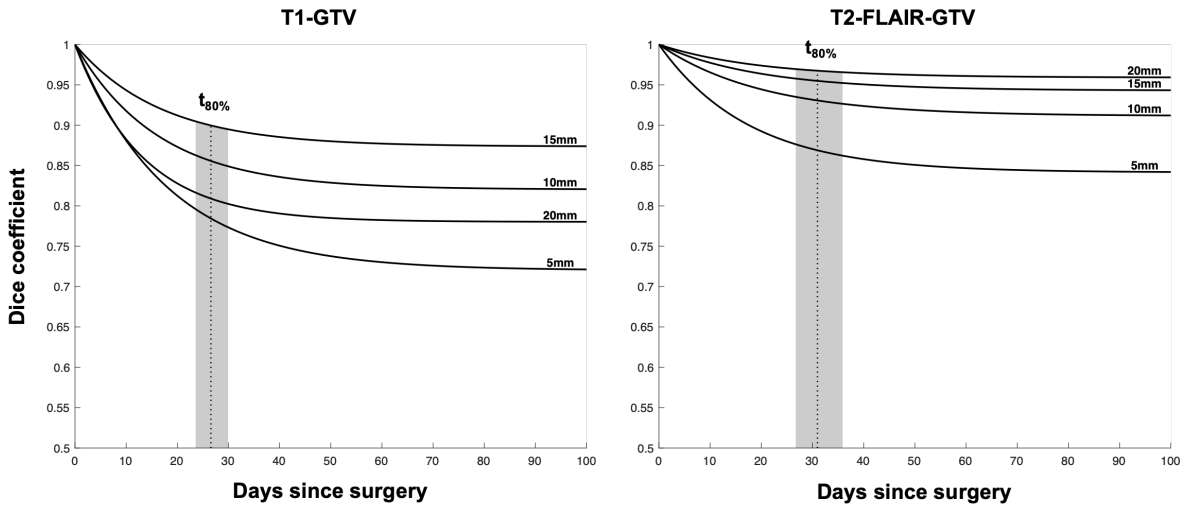

Figure S7. Change in Dice coefficient over time. Dotted vertical lines represent the $t_{80\%}$ with its associated 95% confidence interval.

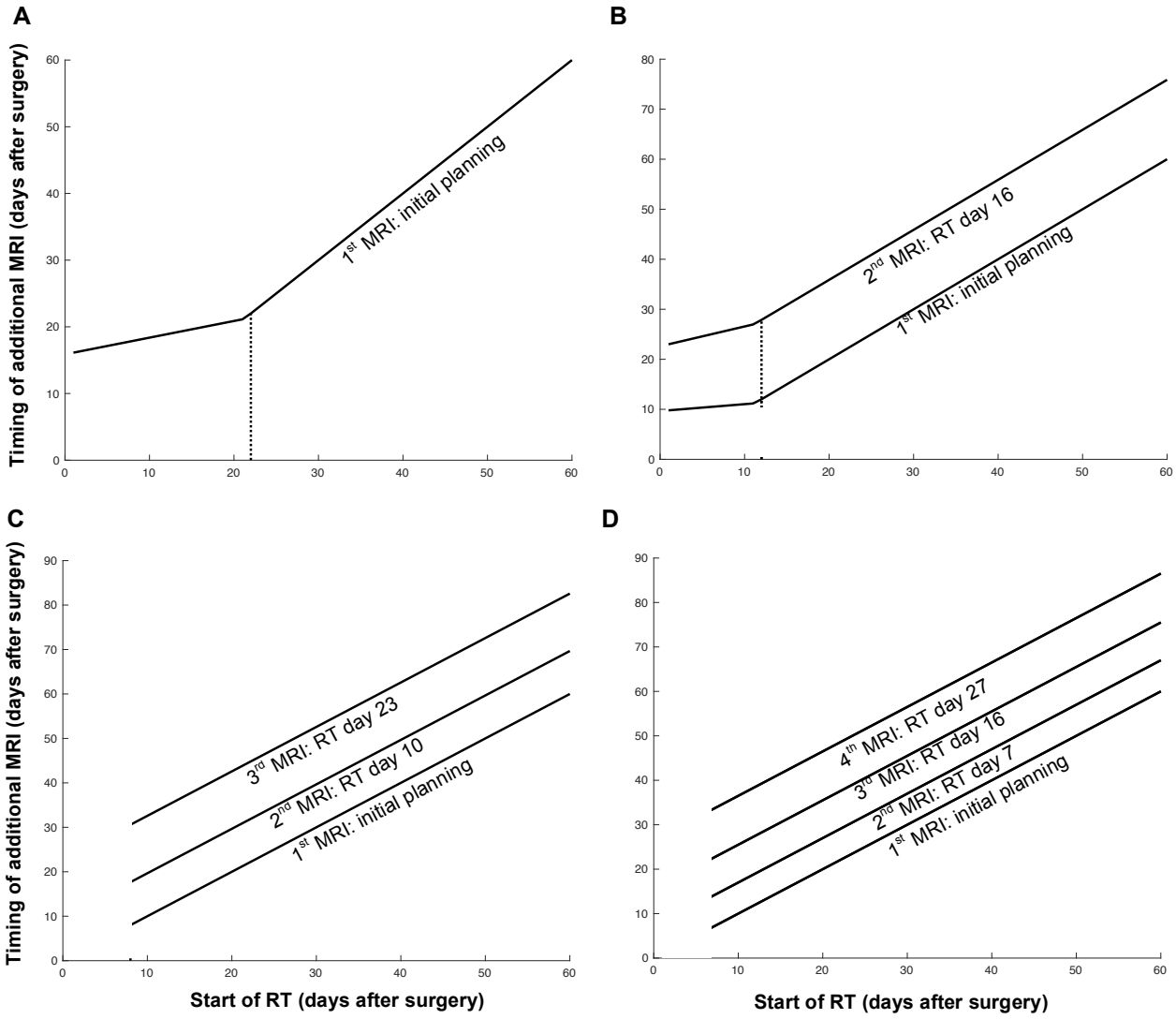

Figure S8. Suggested MRI timing for one (A), two (B), three (C), and four (D) additional MRIs for nCIV reduction. The initial planning MRI is as close to the start of RT as possible. Optimal MRIs for ART are at regular intervals after the start of RT.